Asymptotic Performance of Subspace Methods for Synchronous Multirate CDMA Systems

Zhengyuan Xu, *Senior Member, IEEE*

***Abstract*—Two direct sequence (DS) code division multiple access (CDMA) multirate access methods with a fixed chip rate can be employed to support multirate services: multicode (MC) access and multiple processing gain (MPG) access. In either an MC or an MPG multirate CDMA system, severe intersymbol interference (ISI) may exist due to large channel delay spread relative to the symbol interval. In this paper, we generalize the blind subspace technique to such a multirate CDMA system in order to estimate possibly long channel impulse response of a desired user. Then, we build a blind minimum mean-square-error (MMSE) detector to detect the user's information. The detection performance can be significantly improved by suppressing ISI, which becomes feasible after the user's channel parameters are estimated. The asymptotic performance of the channel estimator and the detector is analyzed. In particular, for typical distributions of the inputs and channel noise, closed-form expressions for the channel estimation error and the output signal-to-interference-plus-noise ratio (SINR) of the detector are derived as functions of the number of received data samples and system parameters. Simulation results are provided to verify our analysis.**

***Index Terms*—Asymptotic analysis, interference suppression, multirate CDMA, subspace decomposition.**

I. Introduction

As a multiple access technique to accommodate multiuser communications, a direct sequence (DS) code division multiple access (CDMA) scheme has been extensively studied for single-rate wireless communication systems [6], [21], [23], [24]. One of the major reasons for its popularity is due to its capability of offering high capacity. However, the third-generation mobile radio systems should be able to provide multimedia services such as voice, image, and data transmissions at different rates. Considerable activities have been conducted on standardization. Several proposals are expected to converge to a global standard [27].

According to all those proposals, the CDMA technique will continue to thrive due to its attractive characteristics such as flexibility in system design and implementation. To deal with multirate information sources, different multirate access schemes can be employed [9], [13] under the CDMA umbrella:

- multicode (MC) access where each high rate user is assigned multiple codes to spread different bits;
- multiple processing gain (MPG, or so-called variable spreading gain—VSG, or variable spreading length—VSL in the literature) access, where each user is assigned one periodic code sequence with period determined by its data rate;
- variable chip rate (VCR) access, where each user is assigned one code sequence with chipping rate determined by its data rate.

However, the VCR scheme introduces extra difficulty to chip synchronization and frequency planning [17]. A constant chip rate is thus more desirable.

Two constant chipping rate access schemes use different strategy in code assignment. In an MC-based system, the data stream from a high rate (HR) user is converted into a series of parallel low rate (LR) streams spread by different code sequences. The MC multirate system is then translated to a single-rate CDMA system with additional virtual users entering the system. Many existing single-rate receivers are thus directly applicable to detect a user. However, its inherent modulation scheme causes detection delay for an HR user. When MPG is adopted, the user's data rate can be easily adapted by changing the length of the code sequence. In this case, information symbols from a HR user suffers from periodically time-varying interference. Those issues impose new challenges in multiuser detection for both multirate CDMA systems. The maximum-likelihood (ML) detector that trades off the performance and complexity [13] has been proposed. Linear detectors with suboptimum performance are very attractive due to low computational complexity. The decorrelating detector [4], [9], [12], [17], the minimum mean-square-error (MMSE) detector [3], [11], [16], [19], successive interference cancellation (IC) [8], and a decision feedback detector [18] have been derived and analyzed.

In this paper, we focus on a multirate CDMA communication system when the multipath delay spread is comparable with or much longer than the bit duration. For example, when IMT-2000 vehicular channel A model is considered [15], the maximum delay spread is about 2.5 μs. If the data rate is 2 Mbps, then the channel spans almost 5 bit periods which causes significant intersymbol interference (ISI). As data rate increases, channel distortion becomes more severe. For such a communication scenario, both MC and MPG multirate CDMA systems are considered and described by a compact input/output data model. Paying close attention to the newly arising channel characteristic, we extend the work for either a single-user [14] or a single-rate CDMA system [1], [2], [20], [24] to a multirate CDMA system in order to estimate the unknown channel parameters of the user of interest. Such a generalized subspace technique employs not only the signature waveform of the current symbol but waveforms of all other symbols from the desired user as well, leading to improved

Manuscript received February 22, 2001; revised April 30, 2002. The associate editor coordinating the review of this paper and approving it for publication was Dr. Naofal M. W. Al-Dhahir.

The author is with the Department of Electrical Engineering, University of California, Riverside, CA 92521 USA (e-mail: dxu@ee.ucr.edu).

Publisher Item Identifier 10.1109/TSP.2002.800383.

estimation performance. Then, we construct an MMSE detector to detect the user of interest based on estimated channel parameters. Beginning with a straightforward receiver structure, we build a bank of MMSE receivers to detect various interfering symbols first and then subtract their contributions from the received data by borrowing the IC idea [8]. In this work, we restrict our attention to the desired user under the assumption that only the channel of that user has been estimated. However, it is desirable to mitigate the multiuser interference (MUI) if channel parameters of other users are available.

In practice, only a finite number of snapshots are collected and processed. Due to large sample effect, there exists perturbations in the estimated data covariance matrix and, thus, in the estimated noise subspace. Based on perturbation analysis [5], [26] and our data model, a closed-form expression of the channel estimation error is derived explicitly as a function of system parameters and the number of snapshots. Moreover, the performance of the MMSE detector is also investigated by examining its output signal-to-interference-plus-noise ratio (SINR) both analytically and experimentally. Various simulation results show that by considering signature waveforms of all symbols from the desired user, the performance of the channel estimator and detector can be significantly improved.

The paper is organized as follows. Section II describes both MC and MPG multirate CDMA systems in one matrix/vector form. A generalized subspace-based channel estimation technique is proposed, and identifiability conditions are discussed in Section III. In addition, in that section, the asymptotic performance of the channel estimator is analyzed. Then, MMSE detectors are proposed, and asymptotic performance is studied in Section IV followed by numerical examples in Section V. Finally, conclusions are drawn in Section VI.

II. Multirate Direct-Sequence CDMA Model

Consider a multirate synchronous CDMA system with K users transmitting their data bits to a common base station through individual multipath fading channel [13]. Suppose the system supports M different data rates. We partition all users into M groups. In group m, assume there are K_m users with data rate R_m. Then, $K = \sum_{m=1}^{M} K_m$. Users in group 1 have the lowest data rate R_1, whereas R_m is a multiple of R_1: $R_m = mR_1$. For notational convenience, denote the kth user in the mth group by user (k, m). The data stream $b_{k,m}(n)$ of user (k, m) is correspondingly partitioned into blocks with each block containing m bits. Denote the jth bit ($j = 0, 1, \ldots, m-1$) in the nth block by $b_{k,m,n}(j) \triangleq b_{k,m}(mn+j)$. Multirate spreading can be achieved by two different code assignment methods [13]. One is to assign m different code sequences of length P_1 to user (k, m), leading to a MC multirate access method. The other one is to assign only one code sequence of length P_m repetitively to each of m bits, where $P_m = P_1/m$, resulting in an MPG multirate access method. In the former, we denote code vector for the jth bit in each block by $\boldsymbol{c}_{k,m,j} = [c_{k,m,j}(0), \ldots, c_{k,m,j}(P_1 - 1)]^T$. In the latter, we denote that common code vector by $\tilde{\boldsymbol{c}}_{k,m} = [\tilde{c}_{k,m}(0), \ldots, \tilde{c}_{k,m}(P_m - 1)]^T$. In order to describe the MC and MPG multirate CDMA systems in a general form, we construct a vector of length P_1 from $\tilde{\boldsymbol{c}}_{k,m}$ by appending some leading and/or tailing zeros to it. Therefore, the code vector for the jth bit has a form $\boldsymbol{e}_j \otimes \tilde{\boldsymbol{c}}_{k,m}$, where $\boldsymbol{e}_j$ is a $m \times 1$ unitary vector with only the jth element nonzero, and "$\otimes$" represents the Kronecker product [10]. In such a way, the code vector $\boldsymbol{c}_{k,m,j}$ adopted for the MC multirate access method can also represent the spreading codes for the MPG multirate access method after setting corresponding elements to be zeros. We will thus use $\boldsymbol{c}_{k,m,j}$ to denote the spreading codes for the jth bit in each block, irrespective of a particular multirate access method.

The user's signal is spread and then propagates through an unknown multipath environment with a finite-length channel impulse response. Assume the channel has order $q_{k,m}$.[1] Together with the transmitter filter and receiver filter, the front-end overall channel impulse response can be described by unknown chip rate coefficients $g_{k,m}(n)$. After considering m bits in each block, the received signal due to user (k, m) becomes [13]

$$y_{k,m}(u) = \sum_{i'=0}^{q_{k,m}} g_{k,m}(i') s_{k,m}(u - i')$$
$$s_{k,m}(u) = \sum_{j=0}^{m-1} \sum_{l=-\infty}^{\infty} b_{k,m,l}(j) c_{k,m,j}(u - lP_1). \quad (1)$$

To explicitly reveal the channel input/output (I/O) relationship, we will employ a matrix representation [21]. Let us collect ν chip samples of $y_{k,m}(u)$ in a vector $\boldsymbol{y}_{k,m}(n)$ from $u = nP_1$ to $u = nP_1 + \nu - 1$. If channel order is factorized by P_1 as $q_{k,m} = \mu_{k,m} P_1 + \beta_{k,m}$, then ν can be chosen as $\nu = QP_1$, where Q satisfies $Q \geq \max_{k,m}(\mu_{k,m} + 2)$. We also arrange channel coefficients in a vector $\boldsymbol{g}_{k,m} = [g_{k,m}(0), \ldots, g_{k,m}(q_{k,m})]^T$. It is assumed to have unit norm $\|\boldsymbol{g}_{k,m}\| = 1$, where the nonunity norm can be absorbed into a complex gain $\alpha_{k,m}$. Under this consideration and after careful arrangement, the convolution in (1) is then written in a matrix form as

$$\boldsymbol{y}_{k,m}(n) = \sum_{j=0}^{m-1} \sum_{i=i_{k,m,0}}^{Q-1} \alpha_{k,m} \boldsymbol{A}_{k,m,i,j} \boldsymbol{g}_{k,m} b_{k,m,n+i}(j)$$
$$\boldsymbol{A}_{k,m,i,j} = \boldsymbol{J}^{iP_1} \boldsymbol{C}_{k,m,j} \quad (2)$$

where the lower limit for i depends on the channel order $i_{k,m,0} = -\mu_{k,m} - 1 + \delta(\beta_{k,m})$ with $\delta(\cdot)$ denoting the Dirac delta function, $\boldsymbol{J}$ is a $\nu \times \nu$ shift-down matrix with all 1s in the first lower diagonal, and $\boldsymbol{C}_{k,m,j}$ is a $\nu \times (q_{k,m} + 1)$ matrix constructed from the code vector $\boldsymbol{c}_{k,m,j}$

$$\boldsymbol{J} = \begin{bmatrix} 0 & & & 0 \\ 1 & & & \\ & \ddots & & \\ 0 & & 1 & 0 \end{bmatrix}$$

$$\boldsymbol{C}_{k,m,j} = \begin{bmatrix} c_{k,m,j}(0) & & \boldsymbol{0} \\ \vdots & \ddots & c_{k,m,j}(0) \\ c_{k,m,j}(P_1 - 1) & & \vdots \\ & \ddots & c_{k,m,j}(P_1 - 1) \\ \boldsymbol{0} & & \boldsymbol{0} \end{bmatrix}. \quad (3)$$

[1]If the knowledge about this order is not available, its upper bound can be used as a substitute.

For notational convenience, we have defined $\boldsymbol{J}^{-1} \triangleq \boldsymbol{J}^T$ and $\boldsymbol{J}^0 = \boldsymbol{I}$ in (2). Premultiplying the signature vector $\boldsymbol{C}_{k,m,j}\boldsymbol{g}_{k,m}$ of $b_{k,m,n}(j)$ by $\boldsymbol{J}^{iP_1}$ will shift this vector up/down by multiples of P_1 positions, resulting in signature vectors of all other bits.

After considering K users in the system and the additive white Gaussian noise (AWGN) $\boldsymbol{v}(n)$, the received data then has the following form:

$$\boldsymbol{y}(n) = \sum_{m=1}^{M} \sum_{k=1}^{K_m} \sum_{j=0}^{m-1} \sum_{i=i_{k,m,0}}^{Q-1} \cdot \alpha_{k,m} \boldsymbol{A}_{k,m,i,j} \boldsymbol{g}_{k,m} b_{k,m,n+i}(j) + \boldsymbol{v}(n). \quad (4)$$

It can be observed that user (k, m) contributes to $\boldsymbol{y}(n)$ a number of intrablock and interblock bits, as indexed by j and i. Define the total number of bits involved in the data vector by $L_{k,m}$. It depends on the order of the channel, the multirate access method, as well as the total number of data samples collected. For example, when the MC multirate access method is used, $L_{k,m} = m(Q - i_{k,m,0})$. Significant number of bits from a user are involved if its multipath channel has a large delay spread. However, signature waveforms of those bits exhibit certain structures. They stem from the convolution of shifted spreading codes with the same channel. This feature will be utilized in our channel estimation next. Without loss of generality, we assume that user $(\overline{k}, \overline{m})$ is our desired user whose channel vector $\boldsymbol{g}_{\overline{k},\overline{m}}$ needs to be estimated.

III. Estimation of Multipath Channel Parameters

There are different approaches to estimate channel parameters. One of the widely used methods is the subspace method [14]. It has been successfully applied to single-rate CDMA systems [2], [24] and has been improved upon based on a subspace intersection idea [22] for a long observation window that is equal to several symbol periods. An extension to multirate CDMA systems is also discussed with some restrictions on the length of the channel. In this section, we will generalize the subspace idea to a multirate CDMA communication system for channel estimation and study the asymptotic performance of the corresponding estimator.

A. Subspace Approach

As is well known, the subspace method employs either the noise subspace or the signal subspace. The signal subspace is also the span of signature waveforms of associated bits in the received data (4). Both subspaces can be obtained from eigenvalue decomposition (EVD) of the covariance of $\boldsymbol{y}(n)$. We denote signature vectors $\boldsymbol{A}_{k,m,i,j}\boldsymbol{g}_{k,m}$ for user (k, m) by $\boldsymbol{s}_{k,m,i,j}$ and assume that they are linearly independent. Collect these vectors in a matrix $\boldsymbol{S}_{k,m}$ column-wise

$$\boldsymbol{S}_{k,m} = [\boldsymbol{s}_{k,m,i,j}], \quad i = i_{k,m,0}, \ldots, Q-1, \quad j = 0, \ldots, m-1 \quad (5)$$

and put all of its information bits in a vector $\boldsymbol{b}_{k,m}(n)$. Under the i.i.d. assumptions on the users' inputs and the noise, the data covariance matrix $\boldsymbol{R} = E\{\boldsymbol{y}(n)\boldsymbol{y}^H(n)\}$ can be computed from (4). If the noise power is σ_v^2, the EVD of $\boldsymbol{R}$ yields[2]

$$\boldsymbol{R} = \boldsymbol{U}_s \boldsymbol{\Lambda}_s \boldsymbol{U}_s^H + \boldsymbol{U}_n \boldsymbol{\Lambda}_n \boldsymbol{U}_n^H, \quad \boldsymbol{\Lambda}_s = \text{diag}\left(\lambda_i^2 + \sigma_v^2\right), \quad \boldsymbol{\Lambda}_n = \sigma_v^2 \boldsymbol{I}. \quad (6)$$

For our desired user, all signature vectors $\boldsymbol{s}_{\overline{k},\overline{m},i,j}$ lie in the signal subspace $\boldsymbol{U}_s$. Thus, they are orthogonal to $\boldsymbol{U}_n$, which leads to [20], [24]

$$\boldsymbol{U}_n^H \boldsymbol{s}_{\overline{k},\overline{m},i,j} = \boldsymbol{U}_n^H \boldsymbol{A}_{\overline{k},\overline{m},i,j} \boldsymbol{g}_{\overline{k},\overline{m}} = \boldsymbol{0}. \quad (7)$$

Equation (7) holds for all possible i and j. Therefore, the subspace method extended to a multirate CDMA system to estimate $\boldsymbol{g}_{\overline{k},\overline{m}}$ becomes

$$\hat{\boldsymbol{g}}_{\overline{k},\overline{m}} = \arg \min_{\|\boldsymbol{x}\|=1} \boldsymbol{x}^H \left[\sum_{i,j} \boldsymbol{A}_{\overline{k},\overline{m},i,j}^H \boldsymbol{U}_n \boldsymbol{U}_n^H \boldsymbol{A}_{\overline{k},\overline{m},i,j} \right] \boldsymbol{x} \quad (8)$$

where i takes integers from $\bar{i}_{\overline{k},\overline{m},0}$ to $Q-1$ and j from 0 to $\overline{m}-1$. For simplicity, we have dropped the limits for them in the summation. We will continue to do so in our later discussion without incurring confusion in the context. Since we restrict our attention to the desired user, we will further skip subscripts $\overline{k}$ and $\overline{m}$ from now on for the same reason. Thus, $\boldsymbol{g}_{\overline{k},\overline{m}}$ and $\boldsymbol{A}_{\overline{k},\overline{m},i,j}$ will be denoted as $\boldsymbol{g}$ and $\boldsymbol{A}_{i,j}$, respectively.

In order to guarantee a unique solution $\hat{\boldsymbol{g}}$, some conditions need to be imposed on system parameters. First, according to (7) and the dimension of the noise subspace, which is $QP_1 - \sum_{m=1}^{M} \sum_{k=1}^{K_m} L_{k,m}$, the following should be satisfied [24];

$$QP_1 - \sum_{m=1}^{M} \sum_{k=1}^{K_m} L_{k,m} \geq q_{\overline{k},\overline{m}} + 1. \quad (9)$$

Other conditions can also be similarly derived by generalizing those for a single-rate CDMA system [21], [24] to the current multirate CDMA system. In the current framework, the desired user creates multiple virtual users. Therefore, there are multiple signature vectors defining the subspace of the signal space of interest, leading to an expanded subspace, as shown by the following theorem.

Theorem [21], [24]: Let $\mathcal{A}$ be a code matrix constructed by stacking $\boldsymbol{A}_{i,j}$ of the desired user for all i and j column by column, and similarly, let $\mathcal{H}_{int}$ be an interference matrix whose columns consist of signature vectors from all other users

$$\mathcal{A} = [\boldsymbol{A}_{i,j}], \qquad \mathcal{H}_{int} = [\boldsymbol{S}_{k,m}].$$

Under (9) and if $[\mathcal{A}, \mathcal{H}_{int}]$ has full column rank, then $\boldsymbol{g}$ is a unique minimum solution of (8) up to a multiplicative scalar. □

By minimizing (8), the solution is then the unique eigenvector of the following objective matrix:

$$\boldsymbol{O} = \sum_{i,j} \boldsymbol{A}_{i,j}^H \boldsymbol{U}_n \boldsymbol{U}_n^H \boldsymbol{A}_{i,j} \quad (10)$$

corresponding to its null eigenvalue. We will study the performance of the proposed channel estimator next when the noise subspace is obtained from the estimated data covariance matrix.

[2]For convenience, we will not specify the dimension for any identity matrix $\boldsymbol{I}$ by dropping its subscript later.

B. Asymptotic Performance of the Channel Estimator

Assume that $\boldsymbol{R}$ is estimated from N data sample vectors [5], [26]

$$\hat{\boldsymbol{R}} = \frac{1}{N}\sum_{n=1}^{N} \boldsymbol{y}(n)\boldsymbol{y}^H(n). \tag{11}$$

The finite data samples will determine the accuracy of the subspace estimate, thus affecting the performance of the estimator. An estimation error[3] $\delta\boldsymbol{R}$ is introduced in estimating $\boldsymbol{R}$ due to finite data samples: $\hat{\boldsymbol{R}} = \boldsymbol{R} + \delta\boldsymbol{R}$. Because of (11), matrix $\delta\boldsymbol{R}$ is Hermitian (complex conjugate symmetric). It can be assumed to be a small perturbation when N is large enough.

For notational convenience, let $\boldsymbol{Z}$ be the noise-free data covariance matrix

$$\boldsymbol{Z} = \boldsymbol{R} - \sigma_v^2\boldsymbol{I} = \boldsymbol{U}_s\boldsymbol{\Omega}\boldsymbol{U}_s^H, \qquad \boldsymbol{\Omega} = \text{diag}\{\lambda_i^2\}. \tag{12}$$

Then, the perturbation of the noise subspace of $\boldsymbol{R}$ has the following form [26]:

$$\delta\boldsymbol{U}_n \approx -\boldsymbol{Z}^\dagger\delta\boldsymbol{R}\boldsymbol{U}_n \tag{13}$$

where $(\cdot)^\dagger$ denotes the pseudoinverse. If a perturbation occurs in estimating $\boldsymbol{U}_n$, then an error will be transferred to our channel estimate. We have shown that $\boldsymbol{g}$ is a unique eigenvector corresponding to the null eigenvalue of $\boldsymbol{O}$. Assume that the perturbation of $\boldsymbol{g}$ is $\delta\boldsymbol{g}$ and that the perturbation of $\boldsymbol{O}$ is $\delta\boldsymbol{O}$. Then, $\delta\boldsymbol{g}$ has the following form [1], [5]:

$$\delta\boldsymbol{g} \approx -\boldsymbol{O}^\dagger\delta\boldsymbol{O}\boldsymbol{g}. \tag{14}$$

According to (10), $\delta\boldsymbol{O}$ is given by

$$\delta\boldsymbol{O} \approx \sum_{i,j} \boldsymbol{A}_{i,j}^H\left[\delta\boldsymbol{U}_n\boldsymbol{U}_n^H + \boldsymbol{U}_n\delta\boldsymbol{U}_n^H\right]\boldsymbol{A}_{i,j}. \tag{15}$$

Substituting (13) in (15), (15) in (14), and noticing (7), we obtain

$$\delta\boldsymbol{g} \approx \sum_{i,j} \boldsymbol{O}^\dagger\boldsymbol{A}_{i,j}^H\boldsymbol{U}_n\boldsymbol{U}_n^H\delta\boldsymbol{R}\boldsymbol{Z}^\dagger\boldsymbol{A}_{i,j}\boldsymbol{g}. \tag{16}$$

Equation (16) shows that $\delta\boldsymbol{g}$ is directly related to $\delta\boldsymbol{R}$, which is random due to the randomness of the received data. Based on this result, the covariance and mean-square-error (MSE) of channel estimate can be further evaluated. The covariance becomes

$$E\{\delta\boldsymbol{g}\delta\boldsymbol{g}^H\} \approx \sum_{i_1,i_2,j_1,j_2} \boldsymbol{O}^\dagger\boldsymbol{A}_{i_1,j_1}^H\boldsymbol{U}_n\boldsymbol{U}_n^H E \cdot\left\{\delta\boldsymbol{R}\boldsymbol{Z}^\dagger\boldsymbol{A}_{i_1,j_1}\boldsymbol{g}\boldsymbol{g}^H\boldsymbol{A}_{i_2,j_2}^H\boldsymbol{Z}^\dagger\delta\boldsymbol{R}\right\}\boldsymbol{U}_n\boldsymbol{U}_n^H\boldsymbol{A}_{i_2,j_2}\boldsymbol{O}^\dagger. \tag{17}$$

To evaluate this quantity, it suffices to determine the following general-form quantity for an arbitrary matrix $\boldsymbol{D}$:

$$\boldsymbol{B} \triangleq E\{\delta\boldsymbol{R}\boldsymbol{D}\delta\boldsymbol{R}\}. \tag{18}$$

This form will also appear in our later discussion on the detector's performance. If $\boldsymbol{D}$ is replaced by $\boldsymbol{Z}^\dagger\boldsymbol{A}_{i_1,j_1}\boldsymbol{g}\boldsymbol{g}^H\boldsymbol{A}_{i_2,j_2}^H\boldsymbol{Z}^\dagger$, then (17) can be easily evaluated. Matrix $\boldsymbol{B}$ depends on the second-order statistics of $\delta\boldsymbol{R}$. Therefore, it relies on up to the fourth-order statistics of the received data since $\delta\boldsymbol{R}$ is related to the second-order information of the channel output. For a single-rate CDMA system, it is shown in [26] that $\boldsymbol{B}$ can be evaluated, as long as the system parameters, distributions of inputs, and channel noise are given. However, to simplify computations and obtain a closed-form expression, we will derive $\boldsymbol{B}$ differently.

For notational convenience, denote $\boldsymbol{y}(n)$ in (4) by $\boldsymbol{y}_n$ and $\boldsymbol{v}(n)$ by $\boldsymbol{v}_n$. Our model (4) can be written in another form:

$$\boldsymbol{y}_n = \boldsymbol{H}\boldsymbol{b}_n + \boldsymbol{v}_n \tag{19}$$

where inputs from all users are collected in a vector $\boldsymbol{b}_n$ whose variance is denoted by $E\{\boldsymbol{b}_n\boldsymbol{b}_n^H\} = \boldsymbol{\Gamma}$, and $\boldsymbol{H}$ is a corresponding signature waveform matrix, including the effect of complex gains $\alpha_{k,m}$. Assume all inputs have zero odd moments, equal variance $E\{|b_{k,m}(n)|^2\} = \sigma_b^2$, and fourth-order absolute moment $E\{|b_{k,m}(n)|^4\} = m_{4b}$. They are also independent of each other, rendering $\boldsymbol{\Gamma}$ a diagonal matrix $\sigma_b^2\boldsymbol{I}$. In the case when users have different transmission power, one can properly scale the complex gain and, thus, the corresponding columns of $\boldsymbol{H}$ to make the power of all users virtually equal for the evaluation purpose. Additionally, we assume that $\boldsymbol{v}_n$ has zero odd moments and is independent of inputs.

It is shown in the Appendix that for a given matrix $\boldsymbol{D}$, waveform matrix $\boldsymbol{H}$, the number N of data vectors, and statistics of inputs and noise, $\boldsymbol{B}$ can always be evaluated according to either (43), when the communication system is a real system (all quantities are real-valued), or (50), when it is a complex system. When applying those results to simplify (17), it is noted that $\boldsymbol{U}_n^H\boldsymbol{B}\boldsymbol{U}_n$ can be first simplified in two cases, respectively.

Case 1—Real System: Since $\boldsymbol{U}_n^H\boldsymbol{U}_n = \boldsymbol{I}$, $\boldsymbol{U}_n$ is orthogonal to both $\boldsymbol{Z}^\dagger$ and $\boldsymbol{H}$, applying (43) yields

$$\boldsymbol{U}_n^H\boldsymbol{B}\boldsymbol{U}_n = \frac{\sigma_v^2}{N}\gamma_{i_1,j_1,i_2,j_2}\boldsymbol{I}$$

where γ_{i_1,j_1,i_2,j_2} is a scalar

$$\gamma_{i_1,j_1,i_2,j_2} = \sigma_b^2\boldsymbol{g}^H\boldsymbol{A}_{i_2,j_2}^H\boldsymbol{Z}^\dagger\boldsymbol{H}\boldsymbol{H}^H\boldsymbol{Z}^\dagger\boldsymbol{A}_{i_1,j_1}\boldsymbol{g} + \sigma_v^2\boldsymbol{g}^H\boldsymbol{A}_{i_2,j_2}^H\boldsymbol{Z}^{\dagger 2}\boldsymbol{A}_{i_1,j_1}\boldsymbol{g}. \tag{20}$$

Since $\boldsymbol{Z} = \sigma_b^2\boldsymbol{H}\boldsymbol{H}^H$ and $\boldsymbol{R} = \boldsymbol{Z} + \sigma_v^2\boldsymbol{I}$, (20) is simplified to

$$\gamma_{i_1,j_1,i_2,j_2} = \boldsymbol{g}^H\boldsymbol{A}_{i_2,j_2}^H\boldsymbol{Z}^\dagger\boldsymbol{R}\boldsymbol{Z}^\dagger\boldsymbol{A}_{i_1,j_1}\boldsymbol{g}. \tag{21}$$

Case 2—Complex System: After applying (50) and observing $\boldsymbol{Z} = \sigma_b^2\boldsymbol{H}\boldsymbol{H}^H$, we obtain

$$\boldsymbol{U}_n^H\boldsymbol{B}\boldsymbol{U}_n = \frac{\sigma_v^2}{N}\gamma_{i_1,j_1,i_2,j_2}\boldsymbol{I}$$

where

$$\gamma_{i_1,j_1,i_2,j_2} = \boldsymbol{g}^H\boldsymbol{A}_{i_2,j_2}^H\boldsymbol{Z}^\dagger\boldsymbol{R}\boldsymbol{Z}^\dagger\boldsymbol{A}_{i_1,j_1}\boldsymbol{g} \tag{22}$$

which is same as (21).

In both cases, (17) becomes

$$E\{\delta\boldsymbol{g}\delta\boldsymbol{g}^H\} \approx \frac{\sigma_v^2}{N}\sum_{i_1,i_2,j_1,j_2}\gamma_{i_1,j_1,i_2,j_2} \cdot\boldsymbol{O}^\dagger\boldsymbol{A}_{i_1,j_1}^H\boldsymbol{U}_n\boldsymbol{U}_n^H\boldsymbol{A}_{i_2,j_2}\boldsymbol{O}^\dagger \tag{23}$$

where γ_{i_1,j_1,i_2,j_2} is given by (21). The MSE of the estimated channel vector is then the trace of matrix $E\{\delta\boldsymbol{g}\delta\boldsymbol{g}^H\}$

$$E\{\|\delta\boldsymbol{g}\|^2\} \approx \frac{\sigma_v^2}{N}\sum_{i_1,i_2,j_1,j_2}\gamma_{i_1,j_1,i_2,j_2} \cdot\text{tr}\left\{\boldsymbol{O}^\dagger\boldsymbol{A}_{i_1,j_1}^H\boldsymbol{U}_n\boldsymbol{U}_n^H\boldsymbol{A}_{i_2,j_2}\boldsymbol{O}^\dagger\right\}. \tag{24}$$

According to (24), it can be observed that the MSE is proportional to σ_v^2/N, which is similar to the result obtained in [1]. Meanwhile, it is determined by projections of code matrices

[3]From now on, we will use $\hat{\cdot}$ to represent the perturbed version of the quantity and a δ preceding the quantity to represent its perturbation.

$\boldsymbol{A}_{i,j}$ of the desired user onto the noise subspace according to the quantity inside the trace operator. If we examine the scalar $\gamma_{i_1, j_1, i_2, j_2}$, we can conclude that the MSE is approximately inversely proportional to the power of the transmitted signal because of the term $\boldsymbol{Z}^\dagger \boldsymbol{R} \boldsymbol{Z}^\dagger$. According to subspace decomposition of $\boldsymbol{Z}$ in (12), $\gamma_{i_1, j_1, i_2, j_2}$ also depends on projections of signature vectors of various bits from the desired user onto the signal subspace.

IV. Detection of the Desired User

In this section, we focus on detection of our desired user $(\overline{k}, \overline{m})$ after its channel vector $\boldsymbol{g}$ has been estimated based on our previously discussed subspace method.

A. Direct MMSE Detection

A linear MMSE detector can be designed by reconstructing the signature waveform of the desired signal. This kind of detector has been proposed and discussed in detail in [3] and [16] for a dual-rate/multirate CDMA system. As we know from our data model (4), there are various bits from the desired user contributed to the received data vector. To simplify the structure of the detector, we detect only the following $\overline{m}$ bits from the current block at each time ($i = 0, j = 0, \ldots, \overline{m} - 1$):

$$\boldsymbol{b}_1(n) = \left[b_{\overline{k}, \overline{m}, n}(0), \ldots, b_{\overline{k}, \overline{m}, n}(\overline{m} - 1)\right]^T.$$

Other options exist by detecting bits from neighboring blocks and then subtracting their contributions from the data vector to improve the detection performance. However, even with our current choice, $\overline{m}$ MMSE detectors are still required

$$\boldsymbol{f}_{0,j} = \hat{\boldsymbol{R}}^{-1} \boldsymbol{A}_{0,j} \hat{\boldsymbol{g}}, \qquad j = 0, \ldots, \overline{m} - 1. \tag{25}$$

Equation (25) provides a standard detection technique. Extensive discussion about the method itself seems unnecessary. However, due to our particular channel estimation method, the performance of these detectors is dependent on the estimated channel parameters and needs to be investigated.

B. Asymptotic Detection Performance

From (25), we observe that the detector depends on j, which is the bit position in the block. Therefore, we need $\overline{m}$ detectors to detect all bits in $\boldsymbol{b}_1(n)$ within the current block. For shorter notation and without confusing the context, we drop the subscripts and denote $\boldsymbol{f}_{0,j}$ and $\boldsymbol{A}_{0,j}$ by $\overline{\boldsymbol{f}}$ and $\overline{\boldsymbol{A}}$, respectively. Keep in mind that they, as well as relevant quantities subsequently defined, are pertaining to a particular bit in $\boldsymbol{b}_1(n)$. An ideal (optimal) MMSE detector after ignoring a positive scalar is the one with ideal covariance matrix and true signature waveform vector $\boldsymbol{f}_o = \boldsymbol{R}^{-1}\overline{\boldsymbol{h}}$, where $\overline{\boldsymbol{h}} = \overline{\boldsymbol{A}}\boldsymbol{g}$. Since the covariance matrix is estimated from data samples with perturbation $\delta\boldsymbol{R}$ and the channel vector has an error from estimation, our detector exhibits degraded performance. We will analyze this loss analytically. First replacing $\hat{\boldsymbol{R}}$ by $\boldsymbol{R} + \delta\boldsymbol{R}$ and $\hat{\boldsymbol{g}}$ by $\boldsymbol{g} + \delta\boldsymbol{g}$ in (25) and then applying Taylor's series expansion to $(\boldsymbol{R} + \delta\boldsymbol{R})^{-1}$ and keeping the first-order terms, it can be found that

$$\overline{\boldsymbol{f}} = \boldsymbol{f}_o + \delta\boldsymbol{f}, \qquad \delta\boldsymbol{f} \approx \boldsymbol{R}^{-1}\overline{\boldsymbol{A}}\delta\boldsymbol{g} - \boldsymbol{R}^{-1}\delta\boldsymbol{R}\boldsymbol{R}^{-1}\overline{\boldsymbol{h}}. \tag{26}$$

Substituting $\delta\boldsymbol{g}$ by (16), $\delta\boldsymbol{f}$ is related to $\delta\boldsymbol{R}$ by

$$\delta\boldsymbol{f} \approx \boldsymbol{R}^{-1}\overline{\boldsymbol{A}}\boldsymbol{O}^\dagger \sum_{i,j} \boldsymbol{A}_{i,j}^H \boldsymbol{U}_n \boldsymbol{U}_n^H \delta\boldsymbol{R} \boldsymbol{Z}^\dagger \boldsymbol{A}_{i,j} \boldsymbol{g} - \boldsymbol{R}^{-1}\delta\boldsymbol{R}\boldsymbol{R}^{-1}\overline{\boldsymbol{h}}. \tag{27}$$

For comparison purposes, we adopt the output SINR as an indicator of the performance of our detector [21]. Define an interference matrix $\boldsymbol{R}_{int} = \boldsymbol{R} - \zeta \overline{\boldsymbol{A}} \boldsymbol{g}\boldsymbol{g}^H \overline{\boldsymbol{A}}^H$, where ζ is the power of the desired user. Then, SINRs of the proposed detector and the ideal MMSE detector can be defined as

$$\begin{aligned} \text{SINR} &= \zeta \frac{E\{\|\overline{\boldsymbol{f}}^H \overline{\boldsymbol{h}}\|^2\}}{E\{\overline{\boldsymbol{f}}^H \boldsymbol{R}_{int} \overline{\boldsymbol{f}}\}} \\ &\approx \zeta \frac{\|\boldsymbol{f}_o^H \overline{\boldsymbol{h}}\|^2 + E\{\delta\boldsymbol{f}^H \overline{\boldsymbol{h}}\,\overline{\boldsymbol{h}}^H \delta\boldsymbol{f}\}}{\boldsymbol{f}_o^H \boldsymbol{R}_{int} \boldsymbol{f}_o + E\{\delta\boldsymbol{f}^H \boldsymbol{R}_{int} \delta\boldsymbol{f}\}} \end{aligned} \tag{28}$$

$$\text{SINR}_o = \zeta \frac{\|\boldsymbol{f}_o^H \overline{\boldsymbol{h}}\|^2}{\boldsymbol{f}_o^H \boldsymbol{R}_{int} \boldsymbol{f}_o}. \tag{29}$$

There are two terms $E\{\delta\boldsymbol{f}^H \overline{\boldsymbol{h}}\,\overline{\boldsymbol{h}}^H \delta\boldsymbol{f}\}$ and $E\{\delta\boldsymbol{f}^H \boldsymbol{R}_{int} \delta\boldsymbol{f}\}$ to be simplified in (28). By direct substitution of (27), they are expanded to

$$\begin{aligned} &E\left\{\delta\boldsymbol{f}^H \overline{\boldsymbol{h}}\,\overline{\boldsymbol{h}}^H \delta\boldsymbol{f}\right\} \\ &\approx \sum_{i_1, i_2, j_1, j_2} \boldsymbol{g}^H \boldsymbol{A}_{i_1, j_1}^H \boldsymbol{Z}^\dagger E\Big\{\delta\boldsymbol{R}\boldsymbol{U}_n \boldsymbol{U}_n^H \boldsymbol{A}_{i_1, j_1} \boldsymbol{O}^\dagger \overline{\boldsymbol{A}}^H \\ &\quad \cdot \boldsymbol{f}_o \boldsymbol{f}_o^H \overline{\boldsymbol{A}} \boldsymbol{O}^\dagger \boldsymbol{A}_{i_2, j_2}^H \boldsymbol{U}_n \boldsymbol{U}_n^H \delta\boldsymbol{R}\Big\} \boldsymbol{Z}^\dagger \boldsymbol{A}_{i_2, j_2} \boldsymbol{g} \\ &\quad - \sum_{i,j} \overline{\boldsymbol{h}}^H \boldsymbol{R}^{-1} E\left\{\delta\boldsymbol{R}\boldsymbol{f}_o \boldsymbol{f}_o^H \overline{\boldsymbol{A}} \boldsymbol{O}^\dagger \boldsymbol{A}_{i,j}^H \boldsymbol{U}_n \boldsymbol{U}_n^H \delta\boldsymbol{R}\right\} \boldsymbol{Z}^\dagger \boldsymbol{A}_{i,j} \boldsymbol{g} \\ &\quad - \sum_{i,j} \boldsymbol{g}^H \boldsymbol{A}_{i,j}^H \boldsymbol{Z}^\dagger E\left\{\delta\boldsymbol{R}\boldsymbol{U}_n \boldsymbol{U}_n^H \boldsymbol{A}_{i,j} \boldsymbol{O}^\dagger \overline{\boldsymbol{A}}^H \boldsymbol{f}_o \boldsymbol{f}_o^H \delta\boldsymbol{R}\right\} \\ &\quad \cdot \boldsymbol{R}^{-1} \overline{\boldsymbol{h}} + \overline{\boldsymbol{h}}^H \boldsymbol{R}^{-1} E\left\{\delta\boldsymbol{R}\boldsymbol{f}_o \boldsymbol{f}_o^H \delta\boldsymbol{R}\right\} \boldsymbol{R}^{-1} \overline{\boldsymbol{h}} \end{aligned} \tag{30}$$

$$\begin{aligned} &E\left\{\delta\boldsymbol{f}^H \boldsymbol{R}_{int} \delta\boldsymbol{f}\right\} \\ &\approx \sum_{i_1, i_2, j_1, j_2} \boldsymbol{g}^H \boldsymbol{A}_{i_1, j_1}^H \boldsymbol{Z}^\dagger E\Big\{\delta\boldsymbol{R}\boldsymbol{U}_n \boldsymbol{U}_n^H \boldsymbol{A}_{i_1, j_1} \boldsymbol{O}^\dagger \overline{\boldsymbol{A}}^H \boldsymbol{G} \\ &\quad \cdot \overline{\boldsymbol{A}} \boldsymbol{O}^\dagger \boldsymbol{A}_{i_2, j_2}^H \boldsymbol{U}_n \boldsymbol{U}_n^H \delta\boldsymbol{R}\Big\} \boldsymbol{Z}^\dagger \boldsymbol{A}_{i_2, j_2} \boldsymbol{g} \\ &\quad - \sum_{i,j} \overline{\boldsymbol{h}}^H \boldsymbol{R}^{-1} E\left\{\delta\boldsymbol{R}\boldsymbol{G}\overline{\boldsymbol{A}} \boldsymbol{O}^\dagger \boldsymbol{A}_{i,j}^H \boldsymbol{U}_n \boldsymbol{U}_n^H \delta\boldsymbol{R}\right\} \boldsymbol{Z}^\dagger \boldsymbol{A}_{i,j} \boldsymbol{g} \\ &\quad - \sum_{i,j} \boldsymbol{g}^H \boldsymbol{A}_{i,j}^H \boldsymbol{Z}^\dagger E\left\{\delta\boldsymbol{R}\boldsymbol{U}_n \boldsymbol{U}_n^H \boldsymbol{A}_{i,j} \boldsymbol{O}^\dagger \overline{\boldsymbol{A}}^H \boldsymbol{G} \delta\boldsymbol{R}\right\} \boldsymbol{R}^{-1} \overline{\boldsymbol{h}} \\ &\quad + \overline{\boldsymbol{h}}^H \boldsymbol{R}^{-1} E\left\{\delta\boldsymbol{R}\boldsymbol{G}\delta\boldsymbol{R}\right\} \boldsymbol{R}^{-1} \overline{\boldsymbol{h}} \end{aligned} \tag{31}$$

where $\boldsymbol{G} = \boldsymbol{R}^{-1} \boldsymbol{R}_{int} \boldsymbol{R}^{-1}$. On the right-hand side of (30) or (31), each term includes a quantity of a typical form $\boldsymbol{B} = E\{\delta\boldsymbol{R}\boldsymbol{D}\delta\boldsymbol{R}\}$, whose expression has been derived analytically in the Appendix for an arbitrary matrix $\boldsymbol{D}$. By setting $\boldsymbol{D}$ equal to the corresponding quantities, all terms can be obtained analytically. Therefore, $E\{\delta\boldsymbol{f}^H \overline{\boldsymbol{h}}\,\overline{\boldsymbol{h}}^H \delta\boldsymbol{f}\}$ and $E\{\delta\boldsymbol{f}^H \boldsymbol{R}_{int} \delta\boldsymbol{f}\}$ can be evaluated. Finally, the expression of SINR follows. These terms are inversely proportional to N. As $N \to \infty$, SINR converges to $SINR_o$ as expected. Unfortunately, different from the channel MSE, the final expression of SINR for a finite N does not exhibit a compact form, even though some terms on the right-hand sides of (30) and (31) can be simplified accordingly.

C. Interference Cancellation (IC)

It has been shown that as far as the desired user is concerned, significant ISI exists in the data vector due to distortion of a relatively long channel. However, signature waveforms of all interfering bits are known at the receiver after the channel of the desired user has been estimated. Motivated by the successive interference cancellation technique [8], we will attempt to successively cancel ISI. By estimating those interfering bits first and subtracting their contributions to the received data vector, it is easily understood that the new detector will provide better performance under certain conditions [8]. This fact motivates us to detect the desired user as follows. Define interfering bit vector $\boldsymbol{b}_1(n+i) = [b_{\overline{k},\overline{m},n+i}(0), \ldots, b_{\overline{k},\overline{m},n+i}(\overline{m}-1)]^T$ in the $(n+i)$th block ($i \neq 0$). First, we design MMSE detectors $\boldsymbol{F}_i$ to detect $\boldsymbol{b}_1(n+i)$ in neighboring blocks. After making decisions based on the outputs of the MMSE detectors and signal constellation, we construct and subtract ISI from $\boldsymbol{y}(n)$. Then, a new data vector is obtained, which is free of ISI if $\boldsymbol{b}_1(n+i)$ are reliably estimated for all $i \neq 0$. We finally build MMSE detectors $\boldsymbol{F}_0$ to detect $\overline{m}$ desired bits in the current block $\boldsymbol{b}_1(n)$. Detailed study on successive interference cancellation has been carried out in the literature, for example, [7] and [8]. It is omitted in the current work due to lack of space. Instead, we will turn our attention to experimental study on the proposed channel estimator and MMSE detector next.

V. SIMULATIONS

We study the performance of our channel estimation and detection methods in different scenarios. A dual-rate synchronous CDMA system is simulated [13]. The first group has two low-rate (LR) users. The second group has two four-fold data rate users. Thus, each high-rate (HR) user creates four virtual users. Although both multirate access schemes are almost equally important, we primarily focus the MPG multirate access method while leaving the MC multirate access scheme only as comparison to minimize redundancy in presentation. For the MPG access, spreading sequences of length 32 are obtained first by adding one random code to the Gold sequences of length 31. Then, each sequence is split into four subsequences to be assigned to each HR user [9]. All users transmit BPSK data symbols at the same power per bit [12]. Twenty one chip spacing channel coefficients for each user are randomly selected from an interval $(-1, 1)$ but fixed in different realizations. Thus, channel response spans about three bit periods of an HR user. Each time $\nu = 96$ chip data samples are collected and processed. Totally, 15–dB background noise is added to the system. The first user in each group is treated as the user of interest, respectively. Therefore, we have a desired LR user and HR user. The channel estimation mean-square-error (MSE) and the output SINR of a detector are adopted as performance measures.

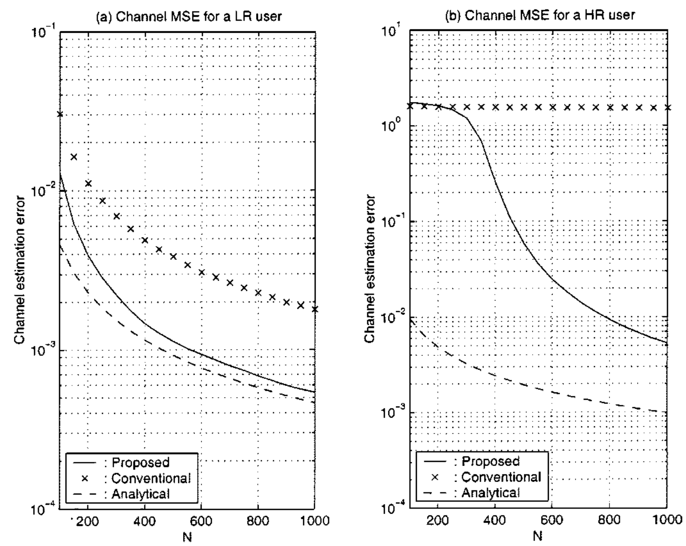

Fig. 1. Data length effect on channel estimation errors.

Fig. 1 investigates the effect of the amount of data record (in terms of N, which is the number of bit periods of the LR user) on the channel estimation error for a LR and HR user, respectively. The average MSE is based on 1000 independent realizations. The solid line represents the proposed method; the "x"s for the conventional subspace method (we define it for convenience), where only the signature waveform of the current bit is used in estimation; and the dashed line from our analytical result. For the LR user, it is observed that the MSE from our method reaches 6×10^{-4} after 1000 bit periods. The experimental result is very close to our analytical results when N is large. The proposed method performs better than the conventional method due to inclusion of signatures of interfering symbols in our cost function. However, for an HR user, the number of interfering symbols in the data vector is much larger than that for a LR user. Therefore, performance differs from that for a LR user, as shown by Fig. 1(b). This time, the conventional method fails to provide a good channel estimate, but the proposed method still works well with increased error level. The difference between the analytical result and the experimental result tends to decrease as N increases. However, it requires more received data vectors for the solid line to converge to the dashed line. Fig. 2 compares the output SINRs of our direct MMSE detector without IC and detector with IC with other detectors such as the decorrelating detector (e.g., [9] and [17]) and RAKE detector (e.g., [11] and [12]). The solid line indicates that with IC, the dashed-dotted line is based on our direct MMSE detection, the "xs" indicate the detector from conventional channel estimation method, the circles are for the decorrelating detector, the diamonds are for the RAKE detector, and the dashed line is our analytical result. For the LR user in Fig. 2(a), we observe that with sufficient received data (after 400 bit periods), the detector with IC outperforms all other detectors. The experimental data from direct MMSE detection is highly consistent with our analytical result. This detector also shows performance similar to the conventional detector due to limited number of interfering bits. Both detectors approach that of the decorrelating detector that uses spreading codes of all users in the system.

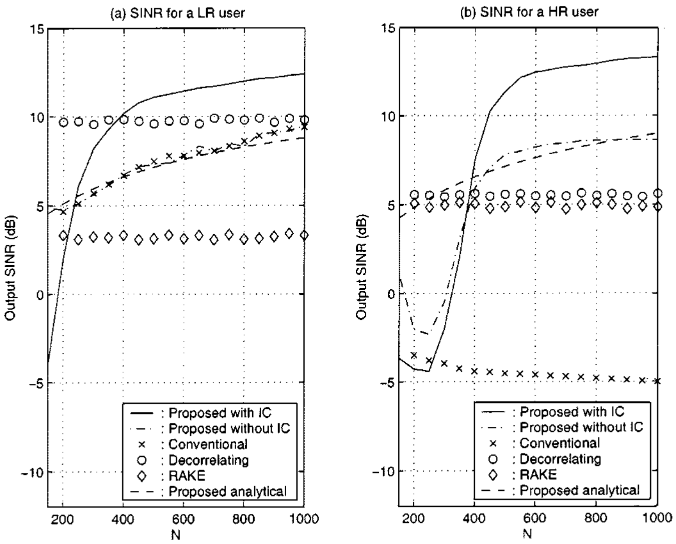

Fig. 2. Near–far effect on output SINR.

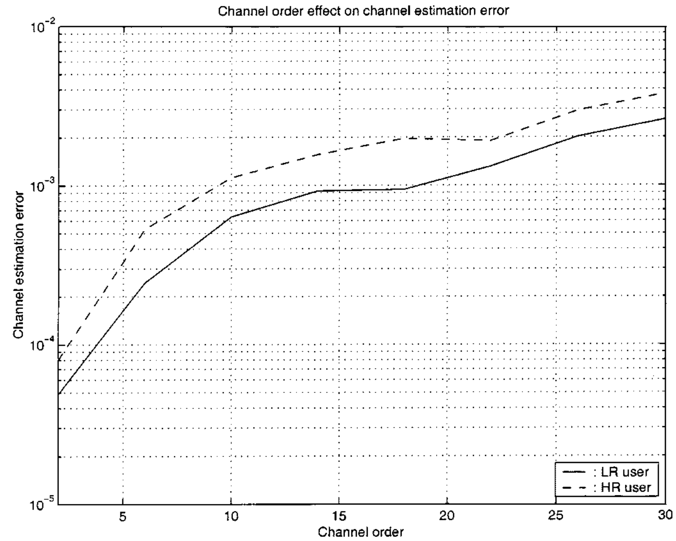

Fig. 3. Effect of sparse channel order on channel estimation errors.

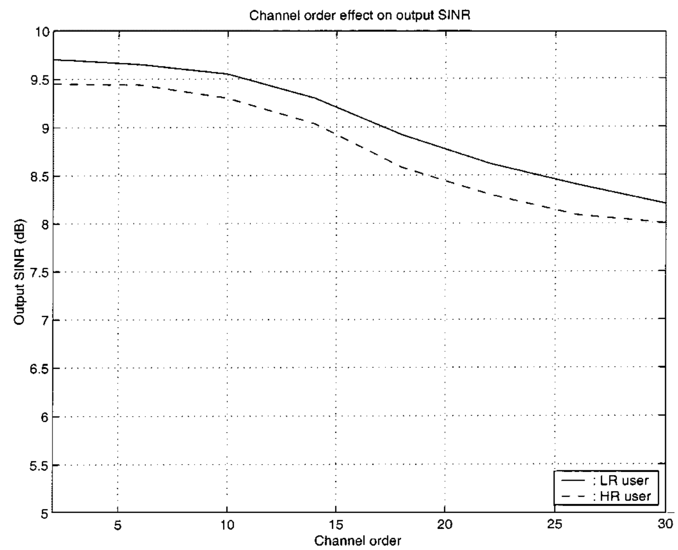

Fig. 4. Effect of sparse channel order on output SINR.

The RAKE detector has the worst performance in this case. For the HR user in Fig. 2(b), after enough data is collected, the direct MMSE detector is better than all other detectors, except the proposed detector with IC. Significant improvement (about 5 dB) is achieved after performing cancellation of ISI. The SINR convergence level is even slightly higher than that of the LR user with IC. The conventional detector is unable to detect the user. The decorrelating and RAKE detectors show similar performance, where SINRs only converge to about 5 dB. It is also observed that even the channel estimation errors are different for both users, as shown in the previous figure; the SINRs are almost indistinguishable for larger N because a relatively reliable channel estimation performance after a certain error level is achieved.

We next study the channel order effect when sparse channels are used. Assume signals from three paths span q chip periods where q varies from 2 to 30. Three nonzero channel coefficients for each user are randomly generated at each realization, and the corresponding channel vector is normalized to have unit norm. The second path arrives with random delay from 1 to $q-1$. The results based on 1000 data vectors are presented in Fig. 3 for the channel MSE and in Fig. 4 for the SINR. All SINR results presented from now on are based on direct MMSE detection unless otherwise specified. From Fig. 3, it is clear that the MSE's for both the LR user and HR user show reliable performance. When q increases to 30, error levels are still below 5×10^{-3}. However, the channel estimation performance for the LR user is better than that for the HR user. After comparing Fig. 3 at $q = 20$ with Fig. 1 at $N = 1000$ for both the LR user and HR user, we can see that the MSEs for such a sparse channel case are comparable with those for the dense channel case. The difference between channel MSEs for users with different data rates does not incur significant difference in SINRs, as observed from Fig. 4. The SINR for the LR user is about 0.5 dB higher than that for the HR user. Both are bounded between 8 and 10 dB for a large range of q. Due to these reasons, we will continue to use dense channels as in Fig. 1 in our later discussion.

We also investigate the effect of rate ratio between the two sets of users. The data rate of two users in the second group is m times that of two users in the first group. Instead of setting $m = 4$ as before, we allow m to take the following integers: $[1, 2, 4, 8, 16]$. Fig. 5 depicts the channel estimation errors for different m, whereas Fig. 6 shows the SINRs. The solid lines are for the desired LR user, and the dashed lines are for the desired HR user. $m = 1$ corresponds to a single-rate CDMA system. As m increases, the MSE for the LR user increases because a significant number of virtual interfering users enter the system. At $m = 16$, each HR user creates 16 virtual users. Hence, the total number of virtual users including LR users in the system reaches 34, giving rise to higher estimation error or lower SINR for the LR user. Regarding to the HR user, the processing gain decreases with increased m. Therefore, the method takes less benefit from spreading, leading to even higher estimation error. The SINR degrades more for the HR user than for the LR user. However, even in such a virtually overloaded system, performance degradation of the proposed method for moderate m is

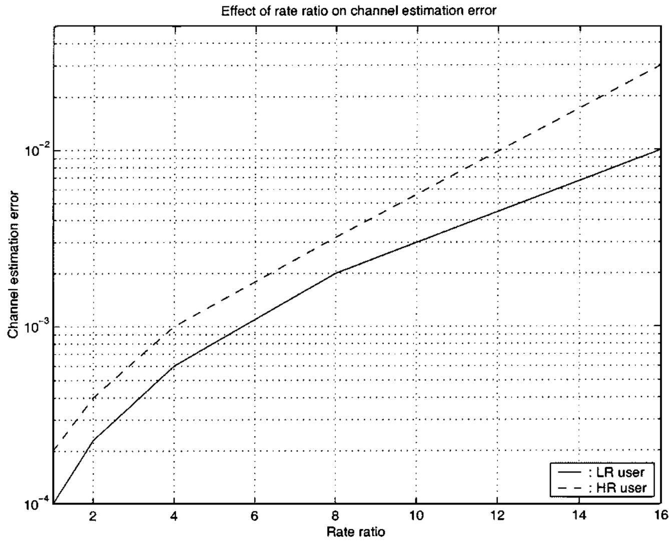

Fig. 5. Effect of rate ratio on channel estimation errors.

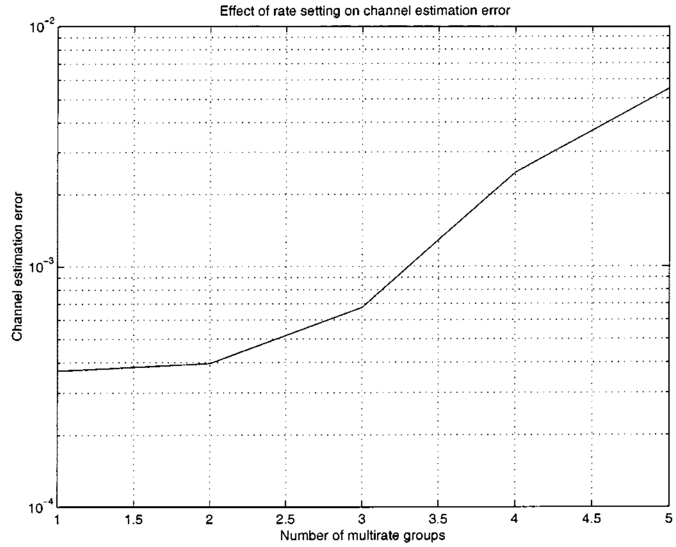

Fig. 7. Effect of number of multiple data rates on channel estimation errors.

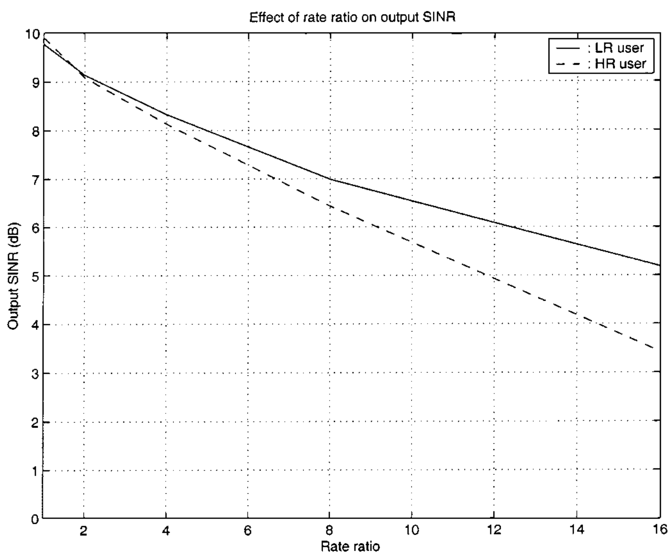

Fig. 6. Effect of rate ratio on output SINR.

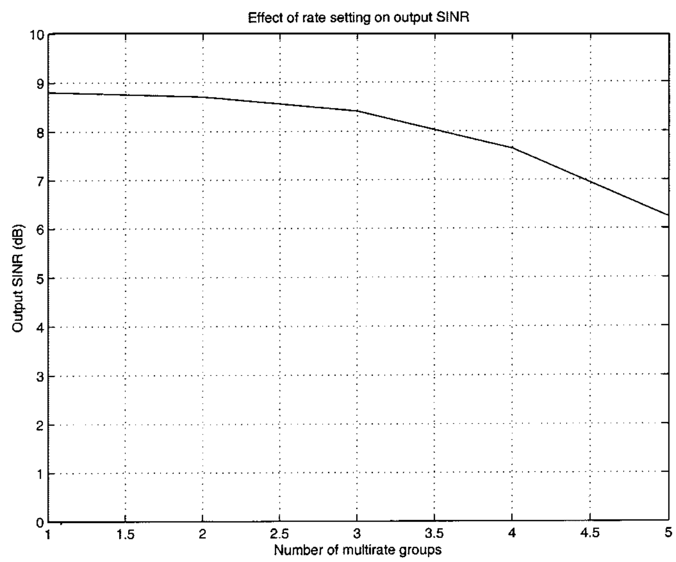

Fig. 8. Effect of number of multiple data rates on output SINR.

tolerable and reasonable. It can also be easily observed that all results at $m = 4$ show consistency correspondingly with those in the first two simulation figures.

The number of data rates existing in a five-user system has a very similar effect on the performance. For convenience, denote the number of data rates by a that can take integers from 1 to 5. Beginning with $a = 1$ corresponding to a single-rate system, we increase a by 1 each time by moving one of five users to a new group and setting its data rate twice of the highest in the previous rate set. Therefore, except for the first group with basic rate R_1, each of the other groups only has one user each time. Under this rate assignment scheme, the highest data rate becomes $16R_1$ when a reaches its maximum 5. One user keeps staying in the first group with the lowest data rate and can be treated as the desired user (LR user). However, there does not exist an HR user for whom the performance is trackable as a varies. As such, the effect of a on the channel estimation error and SINR for the LR user can be examined. They are plotted in Fig. 7 and Fig. 8, respectively. When a is small, both MSE and SINR are relatively insensitive to a change of a since total number of users including virtual users is small. If we regard a user with rate mR_1 as m virtual users, then as a increases, the virtual number of users increases significantly, leading to a higher MSE and lower SINR. However, at $a = 5$, the MSE is about 5×10^{-3}, and the SINR is above 6 dB. After counting the number of virtual users for a different number of multirate groups in Fig. 7 and for different rate ratios in Fig. 5, it is not surprising that the corresponding MSEs for the LR user are in the similar levels. The same conclusion can be made when Figs. 6 and 8 are compared with the x-axes translated to the number of virtual users in both figures. According to this observation, it is clear that the number of virtual users has a significant impact on the performance of the proposed method in the current simulation environment, regardless of whether it stems from multiple data rates or different rate ratios.

The background noise is another factor that affects the performance of our method. Fig. 9 is a typical MSE plot with respect

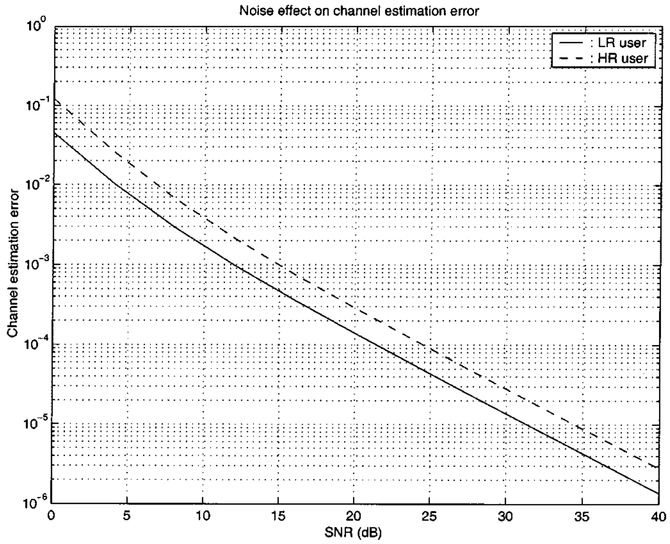

Fig. 9. Noise effect on channel estimation errors.

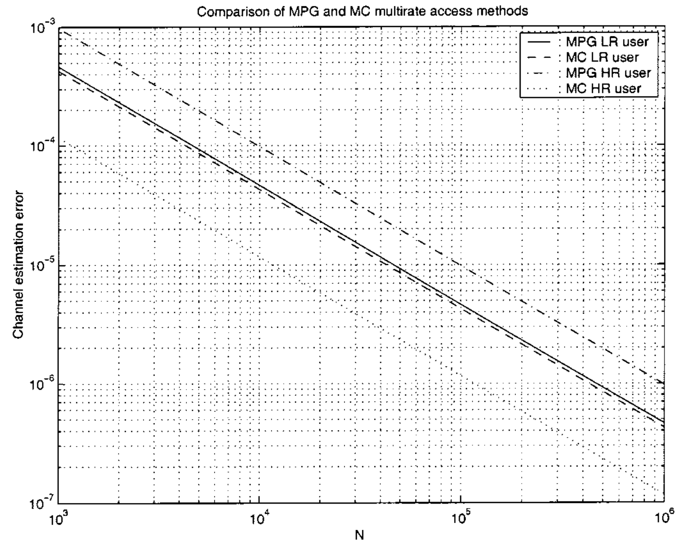

Fig. 11. Channel estimation comparison of the MPG and MC systems.

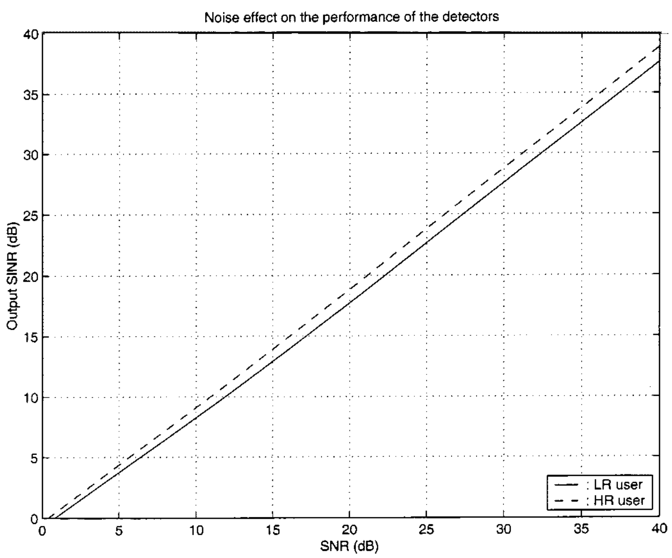

Fig. 10. Noise effect on output SINR.

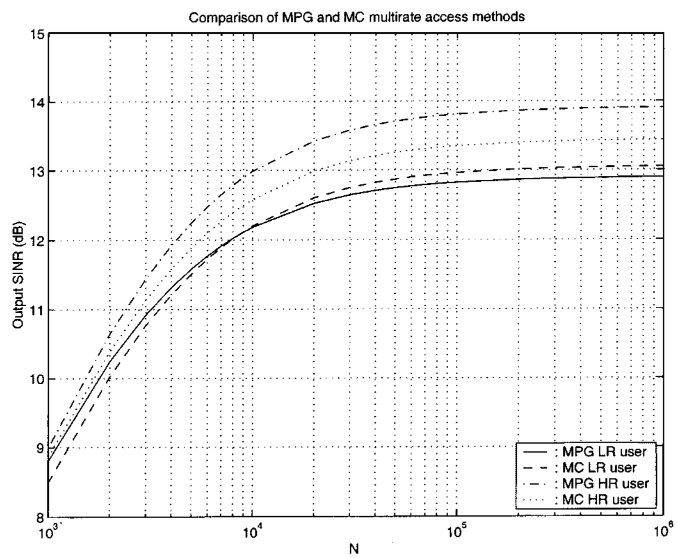

Fig. 12. SINR comparison of the MPG and MC systems.

to signal-to-noise ratios (SNRs) for both the LR and HR users. We vary SNR from 0 to 40 dB by fixing the signal power and changing the noise power only. The performance for the LR user is slightly better than that for the HR user, which is similar to our previous observations. These MSEs change almost linearly with SNR based on the current scales for both axes, indicating that the MSEs are proportional to the noise power, which is consistent with our analysis. Fig. 10 further shows corresponding SINRs with IC. The SINR for the HR user is slightly better than that for the LR user. However, both are very close to SNR at different SNR levels.

Finally, performance of our method in two multirate access systems is compared. The MSEs for both the LR user and HR user are plotted in Fig. 11 with respect to the number of data vectors. For the LR user, the performance under different access methods is comparable, as seen from the solid and dashed lines in the figure, since the same spreading sequence is used for the LR user in both multirate systems. The slight difference might be due to the variation of interference from HR users when different access methods are used. For the HR user, however, our estimation produces much smaller channel MSEs by the MC access method than the MPG method. When the output SINR with IC is examined in Fig. 12, the MPG access method can instead offer improved detection performance over the MC access method for the HR user, which is similar to an observation made in [13], where detailed comparison between MC and MPG methods can be found. Again, the multirate access method has little effect on the SINR for the LR user.

VI. Conclusions

In this paper, a multirate CDMA system with either multicode or multiple processing gain access is studied. Due to high-speed transmissions, the communication channel may have a large delay spread. Therefore, the received data is significantly corrupted by ISI besides multiuser interference. We generalize the subspace method to estimate the multipath parameters by considering projections of signature waveforms of all symbols from the desired user onto the noise subspace, leading to performance improvement over the method that employs only partial signature waveforms. Based on perturbation analysis, the asymptotic channel estimation error is derived in a closed form. Built on the estimated channel parameters, direct MMSE detection is also investigated. The detection performance can be further improved by interference mitigation.

APPENDIX
DERIVATION OF MATRIX $\boldsymbol{B} = E\{\delta \boldsymbol{R} \boldsymbol{D} \delta \boldsymbol{R}\}$

We will proceed differently from [26]. We will also derive closed-form expressions for $\boldsymbol{B}$ with typical distributions of the inputs and noise. Instead of performing a "vec" operation [10] on $\boldsymbol{B}$ first, as in [26], we perform it later as necessary. Substituting $\delta\boldsymbol{R}$ by $\hat{\boldsymbol{R}} - \boldsymbol{R}$, we obtain $\boldsymbol{B} = E\{\hat{\boldsymbol{R}}\boldsymbol{D}\hat{\boldsymbol{R}}\} - \boldsymbol{R}\boldsymbol{D}\boldsymbol{R}$. Assume that N data vectors used in obtaining $\hat{\boldsymbol{R}}$ are mutually independent. Then, $E\{\hat{\boldsymbol{R}}\boldsymbol{D}\hat{\boldsymbol{R}}\} = (1/N)\boldsymbol{G}_1 + (1-(1/N))\boldsymbol{R}\boldsymbol{D}\boldsymbol{R}$, where $\boldsymbol{G}_1 \triangleq E\{\boldsymbol{y}_n\boldsymbol{y}_n^H\boldsymbol{D}\boldsymbol{y}_n\boldsymbol{y}_n^H\}$. Therefore

$$\boldsymbol{B} = \frac{1}{N}(\boldsymbol{G}_1 - \boldsymbol{R}\boldsymbol{D}\boldsymbol{R}). \tag{32}$$

After substituting $\boldsymbol{y}_n$ by (19) and imposing independence among all inputs in $\boldsymbol{b}_n$ and noise $\boldsymbol{v}_n$, it can be found that only the following terms survive in $\boldsymbol{G}_1$:

$$\begin{aligned}\boldsymbol{G}_1 = &\boldsymbol{H}E\left\{\boldsymbol{b}_n\boldsymbol{b}_n^T\right\}\boldsymbol{H}^T\boldsymbol{D}^T E\left\{\boldsymbol{v}_n^*\boldsymbol{v}_n^H\right\}\\ &+E\left\{\boldsymbol{v}_n\boldsymbol{v}_n^T\right\}\boldsymbol{D}^T\boldsymbol{H}^* E\left\{\boldsymbol{b}_n^*\boldsymbol{b}_n^H\right\}\boldsymbol{H}^H\\ &+\sigma_b^2\sigma_v^2\boldsymbol{H}\boldsymbol{H}^H\boldsymbol{D} + \sigma_b^2\sigma_v^2\boldsymbol{D}\boldsymbol{H}\boldsymbol{H}^H\\ &+\sigma_b^2\sigma_v^2\mathrm{tr}(\boldsymbol{H}^H\boldsymbol{D}\boldsymbol{H})\boldsymbol{I} + \sigma_b^2\sigma_v^2\mathrm{tr}(\boldsymbol{D})\boldsymbol{H}\boldsymbol{H}^H\\ &+\boldsymbol{H}E\left\{\boldsymbol{b}_n\boldsymbol{b}_n^H\boldsymbol{H}^H\boldsymbol{D}\boldsymbol{H}\boldsymbol{b}_n\boldsymbol{b}_n^H\right\}\boldsymbol{H}^H\\ &+E\left\{\boldsymbol{v}_n\boldsymbol{v}_n^H\boldsymbol{D}\boldsymbol{v}_n\boldsymbol{v}_n^H\right\}\end{aligned} \tag{33}$$

where "tr" denotes the trace of a matrix, superscript "$*$" denotes complex conjugate, the first two terms result from transposing some scalars ($x^T = x$) in order to reorder corresponding quantities, and $E\{\boldsymbol{v}_n\boldsymbol{v}_n^H\} = \sigma_v^2\boldsymbol{I}$ has been applied. Assume that the length of $\boldsymbol{b}_n$ is L. The last two terms in (33) depend on the fourth-order moments of the source and the noise, respectively. All other terms are either already in evaluative forms or are dependent on the second-order moments. In order to obtain a closed-form expression for $\boldsymbol{B}$, we differentiate two scenarios: The communication system is either real or complex.

Case 1—Real System: In this case, all quantities are real valued. Under our assumptions on the statistics of the inputs and noise, (33) becomes

$$\begin{aligned}\boldsymbol{G}_1 = &\sigma_b^2\sigma_v^2\boldsymbol{H}\boldsymbol{H}^T(\boldsymbol{D}+\boldsymbol{D}^T) + \sigma_b^2\sigma_v^2(\boldsymbol{D}+\boldsymbol{D}^T)\boldsymbol{H}\boldsymbol{H}^T\\ &+\sigma_b^2\sigma_v^2\mathrm{tr}(\boldsymbol{H}^T\boldsymbol{D}\boldsymbol{H})\boldsymbol{I} + \sigma_b^2\sigma_v^2\mathrm{tr}(\boldsymbol{D})\boldsymbol{H}\boldsymbol{H}^T\\ &+\boldsymbol{H}E\left\{\boldsymbol{b}_n\boldsymbol{b}_n^T\boldsymbol{H}^T\boldsymbol{D}\boldsymbol{H}\boldsymbol{b}_n\boldsymbol{b}_n^T\right\}\boldsymbol{H}^T\\ &+E\left\{\boldsymbol{v}_n\boldsymbol{v}_n^T\boldsymbol{D}\boldsymbol{v}_n\boldsymbol{v}_n^T\right\}.\end{aligned} \tag{34}$$

To evaluate the second term to the last, we perform "vec" and then the reverse "unvec" operations

$$\begin{aligned}&E\left\{\boldsymbol{b}_n\boldsymbol{b}_n^T\boldsymbol{H}^T\boldsymbol{D}\boldsymbol{H}\boldsymbol{b}_n\boldsymbol{b}_n^T\right\}\\ &\quad= \mathrm{unvec}\left[E\left\{(\boldsymbol{b}_n\otimes\boldsymbol{b}_n)\left(\boldsymbol{b}_n^T\otimes\boldsymbol{b}_n^T\right)\right\}\mathrm{vec}\left(\boldsymbol{H}^T\boldsymbol{D}\boldsymbol{H}\right)\right]\end{aligned} \tag{35}$$

where properties of "vec"and the Kronecker product "$\otimes$" have been applied [10]. After some straightforward algebra, it can be verified that [25]

$$\begin{aligned}&E\left\{(\boldsymbol{b}_n\otimes\boldsymbol{b}_n)\left(\boldsymbol{b}_n^T\otimes\boldsymbol{b}_n^T\right)\right\}\\ &= (m_{4b}-3\sigma_b^4)\boldsymbol{X}_1 + \sigma_b^4\boldsymbol{X}_2 + \sigma_b^4\mathrm{vec}(\boldsymbol{I})\mathrm{vec}^T(\boldsymbol{I}) + \sigma_b^4\boldsymbol{I}\end{aligned} \tag{36}$$

where $\boldsymbol{X}_1$ is a block diagonal matrix

$$\boldsymbol{X}_1 = \mathrm{diag}\left\{\boldsymbol{a}_1\boldsymbol{a}_1^T, \ldots, \boldsymbol{a}_L\boldsymbol{a}_L^T\right\}$$

$$\boldsymbol{a}_l^T = \left[0, \ldots, 0, \underbrace{1}_{l\mathrm{th}}, 0, \ldots, 0\right]_{1\times L}, \quad \boldsymbol{X}_2 = [\boldsymbol{a}_j\boldsymbol{a}_i^T]_{L\times L}$$

and $\boldsymbol{X}_2$ has been partitioned into $L \times L$ sub-blocks with the (i, j)th sub-block $\boldsymbol{a}_j\boldsymbol{a}_i^T$. Substituting (36) in (35), we obtain

$$E\left\{\boldsymbol{b}_n\boldsymbol{b}_n^T\boldsymbol{H}^T\boldsymbol{D}\boldsymbol{H}\boldsymbol{b}_n\boldsymbol{b}_n^T\right\} = \boldsymbol{G}_2 + \sigma_b^4\mathrm{tr}(\boldsymbol{H}^T\boldsymbol{D}\boldsymbol{H})\boldsymbol{I} + \sigma_b^4\boldsymbol{H}^T\boldsymbol{D}\boldsymbol{H} \tag{37}$$

where

$$\begin{aligned}\boldsymbol{G}_2 = &\left(m_{4b}-3\sigma_b^4\right)\mathrm{unvec}\left[\boldsymbol{X}_1\mathrm{vec}(\boldsymbol{H}^T\boldsymbol{D}\boldsymbol{H})\right]\\ &+\sigma_b^4\mathrm{unvec}\left[\boldsymbol{X}_2\mathrm{vec}(\boldsymbol{H}^T\boldsymbol{D}\boldsymbol{H})\right].\end{aligned}$$

It is observed that $\boldsymbol{G}_2$ has two typical terms unvec$[\boldsymbol{X}_1\mathrm{vec}(\boldsymbol{W})]$ and unvec$[\boldsymbol{X}_2\mathrm{vec}(\boldsymbol{W})]$. Express matrix $\boldsymbol{W}$ explicitly by columns as $[\boldsymbol{w}_1, \ldots, \boldsymbol{w}_L]$, whose jth diagonal element is $w_{j,j}$. Then, according to the definition of $\boldsymbol{X}_1$, we have

$$\begin{aligned}\mathrm{unvec}\left[\boldsymbol{X}_1\mathrm{vec}(\boldsymbol{W})\right] &= [\boldsymbol{a}_1 w_{1,1}, \ldots, \boldsymbol{a}_L w_{L,L}]\\ &= \mathrm{diag}\{w_{1,1}, \ldots, w_{L,L}\} = \boldsymbol{I}\odot\boldsymbol{W}\end{aligned} \tag{38}$$

where "$\odot$" represents element-wise multiplication. Then, $\boldsymbol{I}\odot\boldsymbol{W}$ keeps only the diagonal elements of $\boldsymbol{W}$. According to the definition of $\boldsymbol{X}_2$, the ith block row of vector $\boldsymbol{X}_2\mathrm{vec}(\boldsymbol{W})$ is $\boldsymbol{a}_1\boldsymbol{a}_i^T\boldsymbol{w}_1 + \cdots + \boldsymbol{a}_L\boldsymbol{a}_i^T\boldsymbol{w}_L$, which can be written as $\boldsymbol{a}_1\boldsymbol{w}_1^T\boldsymbol{a}_i + \cdots + \boldsymbol{a}_L\boldsymbol{w}_L^T\boldsymbol{a}_i$. Since $[\boldsymbol{a}_1, \ldots, \boldsymbol{a}_L] = \boldsymbol{I}$, it becomes $\boldsymbol{W}^T\boldsymbol{a}_i$. Therefore

$$\mathrm{unvec}\left[\boldsymbol{X}_2\mathrm{vec}(\boldsymbol{W})\right] = [\boldsymbol{W}^T\boldsymbol{a}_1, \ldots, \boldsymbol{W}^T\boldsymbol{a}_L] = \boldsymbol{W}^T. \tag{39}$$

With (38) and (39), (37) becomes

$$\begin{aligned}&E\left\{\boldsymbol{b}_n\boldsymbol{b}_n^T\boldsymbol{H}^T\boldsymbol{D}\boldsymbol{H}\boldsymbol{b}_n\boldsymbol{b}_n^T\right\}\\ &\quad= (m_{4b}-3\sigma_b^4)\boldsymbol{I}\odot(\boldsymbol{H}^T\boldsymbol{D}\boldsymbol{H}) + \sigma_b^4\mathrm{tr}(\boldsymbol{H}^T\boldsymbol{D}\boldsymbol{H})\boldsymbol{I}\\ &\qquad+\sigma_b^4\boldsymbol{H}^T(\boldsymbol{D}+\boldsymbol{D}^T)\boldsymbol{H}.\end{aligned} \tag{40}$$

Similar to (40), the last term in (34) is simplified to

$$\begin{aligned}&E\left\{\boldsymbol{v}_n\boldsymbol{v}_n^T\boldsymbol{D}\boldsymbol{v}_n\boldsymbol{v}_n^T\right\}\\ &\quad= (m_{4v}-3\sigma_v^4)\boldsymbol{I}\odot\boldsymbol{D} + \sigma_v^4\mathrm{tr}(\boldsymbol{D})\boldsymbol{I} + \sigma_v^4(\boldsymbol{D}+\boldsymbol{D}^T)\end{aligned} \tag{41}$$

where m_{4v} is the fourth-order absolute moment of the AWGN and is equal to $3\sigma_v^4$. Equation (41) becomes

$$E\left\{\boldsymbol{v}_n\boldsymbol{v}_n^T\boldsymbol{D}\boldsymbol{v}_n\boldsymbol{v}_n^T\right\} = \sigma_v^4\mathrm{tr}(\boldsymbol{D})\boldsymbol{I} + \sigma_v^4(\boldsymbol{D}+\boldsymbol{D}^T). \tag{42}$$

Observe that $\boldsymbol{R} = \sigma_b^2 \boldsymbol{H}\boldsymbol{H}^T + \sigma_v^2 \boldsymbol{I}$. Substituting (40) and (42) in (34) first and then (34) in (32), we obtain

$$\begin{aligned}\boldsymbol{B} = &\frac{\sigma_b^2\sigma_v^2}{N}\left[\boldsymbol{H}\boldsymbol{H}^T\boldsymbol{D}^T + \boldsymbol{D}^T\boldsymbol{H}\boldsymbol{H}^T\right.\\ &\qquad\left. + \operatorname{tr}(\boldsymbol{H}^T\boldsymbol{D}\boldsymbol{H})\boldsymbol{I} + \operatorname{tr}(\boldsymbol{D})\boldsymbol{H}\boldsymbol{H}^T\right]\\ &+ \frac{\sigma_v^4}{N}\left[\boldsymbol{D}^T + \operatorname{tr}(\boldsymbol{D})\boldsymbol{I}\right]\\ &+ \frac{\sigma_b^4}{N}\left[\operatorname{tr}(\boldsymbol{H}^T\boldsymbol{D}\boldsymbol{H})\boldsymbol{H}\boldsymbol{H}^T + \boldsymbol{H}\boldsymbol{H}^T\boldsymbol{D}^T\boldsymbol{H}\boldsymbol{H}^T\right]\\ &+ (m_{4b} - 3\sigma_b^4)\frac{1}{N}\boldsymbol{H}[\boldsymbol{I}\odot(\boldsymbol{H}^T\boldsymbol{D}\boldsymbol{H})]\boldsymbol{H}^T. \qquad (43)\end{aligned}$$

Case 2—Complex System: In this case, the real and imaginary parts of inputs are assumed to be independent and have the same distributions. Similar assumptions are made on the noise. Then, $E\{\boldsymbol{b}_n\boldsymbol{b}_n^T\} = \boldsymbol{0}$ and $E\{\boldsymbol{v}_n\boldsymbol{v}_n^T\} = \boldsymbol{0}$. Equation (33) becomes

$$\begin{aligned}\boldsymbol{G}_1 = &\sigma_b^2\sigma_v^2\boldsymbol{H}\boldsymbol{H}^H\boldsymbol{D} + \sigma_b^2\sigma_v^2\boldsymbol{D}\boldsymbol{H}\boldsymbol{H}^H\\ &+ \sigma_b^2\sigma_v^2\operatorname{tr}(\boldsymbol{H}^H\boldsymbol{D}\boldsymbol{H})\boldsymbol{I} + \sigma_b^2\sigma_v^2\operatorname{tr}(\boldsymbol{D})\boldsymbol{H}\boldsymbol{H}^H\\ &+ \boldsymbol{H}E\left\{\boldsymbol{b}_n\boldsymbol{b}_n^H\boldsymbol{H}^H\boldsymbol{D}\boldsymbol{H}\boldsymbol{b}_n\boldsymbol{b}_n^H\right\}\boldsymbol{H}^H\\ &+ E\left\{\boldsymbol{v}_n\boldsymbol{v}_n^H\boldsymbol{D}\boldsymbol{v}_n\boldsymbol{v}_n^H\right\}. \qquad (44)\end{aligned}$$

As in *Case 1*, we can obtain

$$\begin{aligned}&E\left\{\boldsymbol{b}_n\boldsymbol{b}_n^H\boldsymbol{H}^H\boldsymbol{D}\boldsymbol{H}\boldsymbol{b}_n\boldsymbol{b}_n^H\right\}\\ &\quad= \operatorname{unvec}\left[E\left\{(\boldsymbol{b}_n^*\otimes\boldsymbol{b}_n)\left(\boldsymbol{b}_n^T\otimes\boldsymbol{b}_n^H\right)\right\}\operatorname{vec}(\boldsymbol{H}^H\boldsymbol{D}\boldsymbol{H})\right] \qquad (45)\\ &E\left\{(\boldsymbol{b}_n^*\otimes\boldsymbol{b}_n)\left(\boldsymbol{b}_n^T\otimes\boldsymbol{b}_n^H\right)\right\}\\ &\quad= \left(m_{4b} - 2\sigma_b^4\right)\boldsymbol{X}_1 + \sigma_b^4\operatorname{vec}(\boldsymbol{I})\operatorname{vec}^T(\boldsymbol{I}) + \sigma_b^4\boldsymbol{I}. \qquad (46)\end{aligned}$$

Notice that (46) is different from (40) because of complex inputs. Substituting (46) in (45), and noticing (38), we obtain

$$\begin{aligned}E\left\{\boldsymbol{b}_n\boldsymbol{b}_n^H\boldsymbol{H}^H\boldsymbol{D}\boldsymbol{H}\boldsymbol{b}_n\boldsymbol{b}_n^H\right\} = &\left(m_{4b} - 2\sigma_b^4\right)\boldsymbol{I}\odot(\boldsymbol{H}^H\boldsymbol{D}\boldsymbol{H})\\ &+\sigma_b^4\operatorname{tr}(\boldsymbol{H}^H\boldsymbol{D}\boldsymbol{H})\boldsymbol{I} + \sigma_b^4\boldsymbol{H}^H\boldsymbol{D}\boldsymbol{H}. \qquad (47)\end{aligned}$$

Similarly, we obtain

$$E\left\{\boldsymbol{v}_n\boldsymbol{v}_n^H\boldsymbol{D}\boldsymbol{v}_n\boldsymbol{v}_n^H\right\} = (m_{4v} - 2\sigma_v^4)\boldsymbol{I}\odot\boldsymbol{D} + \sigma_v^4\operatorname{tr}(\boldsymbol{D})\boldsymbol{I} + \sigma_v^4\boldsymbol{D}. \qquad (48)$$

For a complex symmetric Gaussian random variable, m_{4v} equals $2\sigma_v^4$ instead of $3\sigma_v^4$ in the real case (for example, see explanations between [25, eq. (104) and eq. (105)]). Then, (48) becomes

$$E\left\{\boldsymbol{v}_n\boldsymbol{v}_n^H\boldsymbol{D}\boldsymbol{v}_n\boldsymbol{v}_n^H\right\} = \sigma_v^4\operatorname{tr}(\boldsymbol{D})\boldsymbol{I} + \sigma_v^4\boldsymbol{D}. \qquad (49)$$

Observe that $\boldsymbol{R} = \sigma_b^2\boldsymbol{H}\boldsymbol{H}^H + \sigma_v^2\boldsymbol{I}$. Substituting (47) and (49) in (44) first and then (44) in (32), we obtain

$$\begin{aligned}\boldsymbol{B} = &\frac{\sigma_b^2\sigma_v^2}{N}\left[\operatorname{tr}(\boldsymbol{H}^H\boldsymbol{D}\boldsymbol{H})\boldsymbol{I} + \operatorname{tr}(\boldsymbol{D})\boldsymbol{H}\boldsymbol{H}^H\right]\\ &+ \frac{\sigma_v^4}{N}\operatorname{tr}(\boldsymbol{D})\boldsymbol{I} + \frac{\sigma_b^4}{N}\operatorname{tr}(\boldsymbol{H}^H\boldsymbol{D}\boldsymbol{H})\boldsymbol{H}\boldsymbol{H}^H\\ &+ \left(m_{4b} - 2\sigma_b^4\right)\frac{1}{N}\boldsymbol{H}[\boldsymbol{I}\odot(\boldsymbol{H}^H\boldsymbol{D}\boldsymbol{H})]\boldsymbol{H}^H \qquad (50)\end{aligned}$$

which concludes our derivation. □

Acknowledgment

The author would like to thank the anonymous reviewers for valuable comments.

References

[1] E. Aktas and U. Mitra, "Complexity reduction in subspace-based blind channel identification for DS/CDMA systems," *IEEE Trans. Commun.*, vol. 48, pp. 1392–1404, Aug. 2000.
[2] S. Bensley and B. Aazhang, "Subspace-based channel estimation for code division multiple access communication systems," *IEEE Trans. Commun.*, pp. 1009–1020, Aug. 1996.
[3] S. Buzzi, M. Lops, and A. Tulino, "Blind adaptive multiuser detection for asynchronous dual-rate DS/CDMA systems," *IEEE J. Select. Areas Commun.*, vol. 19, pp. 233–244, Feb. 2001.
[4] J. Chen and U. Mitra, "Analysis of decorrelator-based receivers for multirate DS/CDMA communications," *IEEE Trans. Veh. Technol.*, vol. 48, pp. 1966–1983, Nov. 1999.
[5] B. Friedlander and A. Weiss, "On the second-order statistics of the eigenvectors of sample covariance matrices," *IEEE Trans. Signal Processing*, vol. 46, pp. 3136–3139, Nov. 1998.
[6] M. Honig, U. Madhow, and S. Verdu, "Blind adaptive multiuser detection," *IEEE Trans. Inform. Theory*, vol. 41, pp. 944–960, July 1995.
[7] A. Hui and K. Letaief, "Successive interference cancellation for multi-user asynchronous DS/CDMA detectors in multipath fading links," *IEEE Trans. Commun.*, vol. 46, pp. 384–391, Mar. 1998.
[8] A. Johansson and A. Svensson, "On multirate DS-CDMA schemes with interference cancellation," *Wireless Pers. Commun.*, vol. 9, no. 1, pp. 1–29, Jan. 1999.
[9] M. Juntti, "Performance of multiuser detection in multirate CDMA systems," *Wireless Pers. Commun.*, vol. 11, no. 3, pp. 293–311, Dec. 1999.
[10] P. Lancaster and M. Tismenetsky, *The Theory of Matrices*, 2nd ed. San Diego, CA: Academic, 1985.
[11] J. Ma and H. Ge, "Modified multi-rate detection for frequency selective Rayleigh fading CDMA channels," in *Proc. PIMRC*, vol. 3, Boston, MA, Sept. 8–11, 1998, pp. 1304–1308.
[12] M. Madkour and S. Gupta, "Performance analysis of a wireless multirate direct-sequence CDMA using fast walsh transform and decorrelating detection," *IEEE Trans. Commun.*, vol. 48, pp. 1405–1412, Aug. 2000.
[13] U. Mitra, "Comparison of maximum-likelihood-based detection for two multirate access schemes for CDMA signals," *IEEE Trans. Commun.*, vol. 47, pp. 64–77, Jan. 1999.
[14] E. Moulines, P. Duhamel, J.-F. Cardoso, and S. Mayrargue, "Subspace methods for the blind identification of multichannel FIR filters," *IEEE Trans. Signal Processing*, vol. 43, pp. 516–525, Feb. 1995.
[15] T. Ojanpera and R. Prasad, *Wideband CDMA and Third Generation Mobile Communications*. Boston, MA: Artech House, 1998.
[16] A. Sabharwal, U. Mitra, and R. Moses, "MMSE receivers for multirate DS-CDMA systems," *IEEE Trans. Commun.*, vol. 49, pp. 2184–2197, Dec. 2001.
[17] M. Saquib, R. Yates, and N. Mandayam, "Decorrelating detectors for a dual rate synchronous DS/CDMA channel," *Wireless Pers. Commun.*, vol. 9, no. 3, pp. 197–216, May 1999.
[18] ——, "A decision feedback decorrelator for a dual rate synchronous DS/CDMA system," *ACM Wireless Networks*, vol. 4, no. 6, pp. 497–506, 1998.
[19] R. Srinivasan, U. Mitra, and R. Moses, "Design and analysis of receiver filters for multiple chip-rate DS-CDMA systems," *IEEE J. Select. Areas Commun.*, vol. 17, pp. 2096–2109, Dec. 1999.

[20] M. Torlak and G. Xu, "Blind multiuser channel estimation in asynchronous CDMA systems," *IEEE Trans. Signal Processing*, vol. 45, pp. 137–147, Jan. 1997.

[21] M. Tsatsanis and Z. Xu, "Performance analysis of minimum variance CDMA receivers," *IEEE Trans. Signal Processing*, vol. 46, pp. 3014–3022, Nov. 1998.

[22] A. J. Van Der Veen, "Blind subspace-based uplink receiver algorithm for wideband CDMA," in *Proc. IEEE VTS 50th Veh. Technol. Conf.*, vol. 1, Amsterdam, Netherlands, Sept. 19–22, 1999, pp. 176–180.

[23] S. Verdu, *Multiuser Detection*. New York: Cambridge Univ. Press, 1998.

[24] X. Wang and H. Poor, "Blind equalization and multiuser detection in dispersive CDMA channels," *IEEE Trans. Commun.*, vol. 46, pp. 91–103, Jan. 1998.

[25] Z. Xu, "Asymptotically near-optimal blind estimation of multipath CDMA channels," *IEEE Trans. Signal Processing*, vol. 49, pp. 2003–2017, Sept. 2001.

[26] N. Yuen and B. Friedlander, "Asymptotic performance analysis for signature waveform estimation in synchronous CDMA systems," *IEEE Trans. Signal Processing*, vol. 46, pp. 1753–1757, June 1998.

[27] M. Zeng, A. Annamalai, and V. Bhargava, "Harmonization of global third-generation mobile systems," *IEEE Commun. Mag.*, pp. 94–104, Dec. 2000.

Zhengyuan Xu (S'97–M'99–SM'02) received the B.E. and M.E. degrees in electronic engineering from Tsinghua University, Beijing, China, in 1989 and 1991, respectively, and the Ph.D. degree in electrical engineering from Stevens Institute of Technology, Hoboken, NJ, in 1999.

From 1991 to 1996, he was an Engineer and Department Manager at the Tsinghua Unisplendour Group Corporation, Tsinghua University. From 1996 to 1999, he was a Research Assistant and Research Associate with Stevens Institute of Technology, where he worked on signal processing for wireless communications, especially for multiuser CDMA systems. In 1999, he joined the Department of Electrical Engineering, University of California, Riverside, as an Assistant Professor. His current research interests include advanced signal processing, multirate communication, multiuser detection, and system identification.

Dr. Xu received the Outstanding Student Award and the Motorola Scholarship from Tsinghua University and the Peskin Award from Stevens Institute of Technology. He also received the Academic Senate Research Award and the Regents' Faculty Award from University of California, Riverside.